

Theory of Hysteresis Loop in Ferromagnets

Igor F.Lyuksyutov^{a,*}, Thomas Nattermann^b, and Valery Pokrovsky^{a,c}

(a) *Department of Physics, Texas A&M University, College Station, TX 77843-4242*

(b) *Institut für Theoretische Physik, Universität zu Köln, 50937, Köln, Germany*

(c) *Landau Institute for Theoretical Physics, Moscow, Russia*

(December 2, 2024)

Abstract

A theory of the hysteresis loop in ferromagnets controlled by the domain wall motion is presented. Domain walls are considered as plane or linear interfaces moving in a random medium under the action of the external ac magnetic field $H = H_0 \sin \omega t$. We introduce important characteristics of the hysteresis loop, such as dynamic threshold fields, reversal field etc. together with well known characteristics as coercive field and hysteresis loop area (HLA) \mathcal{A} . We show that all these characteristics are regulated by two dimensionless combinations of the H_0 and ω and intrinsic characteristics of the ferromagnet. The moving domain wall can create magnetic bubbles playing the role of pre-existing nuclei of the reversed magnetization. We discuss a simple model of this process. For magnetization reversal determined by domain inflation we predict that HLA scales as $\mathcal{A} \propto \omega^\beta H_0^\alpha$ with $\alpha = 1/2$ and $\beta = 1/2$. Numerical simulations confirm this result.

75.60.Ej,75.70.Ak,75.60.Ch

Magnetic hysteresis loops (HL) have been first studied already more than a century ago [1]. However, the understanding of this process in thin magnetic films is still rather poor. Many efforts have been devoted recently to the prediction [2–5] and experimental verification [6–8] of the scaling behavior of the *hysteresis loop area* (HLA) as a function of the frequency and amplitude of the applied magnetic field in thin magnetic films [8]. The scaling behavior of the HLA has been first reported in the pioneering work [1] for 3D magnets. While there exists an extended literature on the hysteresis of 3D magnets, the properties of the HL in 2D systems are much less known [6–10]. Critical exponents found in the experiments with thin films differ dramatically for different materials [6–8] and probably for different regimes. Different authors disagree with each other [6–8] and also disagree with numerical simulations [2].

More recently mean field type models with single [9] or many [10] relaxation times have been applied to analyze the experimental data for the description of the HL controlled by nucleation processes. These authors predict a logarithmic dependence of the coercive field H_c on the rate of the applied magnetic field \dot{H} . In a recent experiment [8] it was found that the HLA depends on frequency ω of the applied field as power with a small exponent α ($\sim 0.03 – 0.06$) or, possibly, logarithmically. In the framework of the same approach the HLA must behave also logarithmically in H . However, such a dependence has never been observed experimentally.

In this article we propose a new analysis of the HL by formulating a rather general approach to the magnetization reversal mechanisms. In particular, we indicate several important measurable characteristics of the HL besides of the HLA. It turns out, that these characteristics are governed by two dimensionless parameters combined from the field frequency ω , its amplitude H_0 and characteristics of the magnetic material. Everywhere in what follows we assume that the external field varies harmonically in time, $H(t) = H_0 \sin \omega t$.

In general, hysteresis behavior may have various origins. It can be mediated by nucleation processes, by the domain wall (DW) propagation or simply by retardation of the magnetization due to fluctuations. In this article we will restrict ourselves to the second

mechanism, i.e. the hysteretic behavior due to the finite velocity of the DW propagation, and establish conditions at which it is dominant. Discussion of other mechanisms as well as a more detailed presentation of the results of this paper will be postponed to a future publication [11].

We consider magnets of Ising (uniaxial) symmetry. Their properties may be very different depending of the strength of the anisotropy. In the experimentally studied films the anisotropy was very weak. In this case the domain wall width is large in comparison to the lattice constant. On the contrary, in the original Ising model the anisotropy is assumed to be large and DW width l is simply the lattice constant. However, these different models becomes equivalent after a simple rescaling: the DW width should be accepted as a new elementary (cut-off) length. It means that we consider a spin cluster of the linear size l as a new elementary spin.

Disorder plays an important role in the DW propagation: it creates a finite threshold value H_p the external field has to overcome to move the DW and lowers the DW velocity considerably in the low-field regime, $(H - H_p) \ll H_p$, where the DW motion shows critical behavior [12,13]. Peculiarities of the two-dimensional situation are: much higher mobility of the DW as well as much stronger fluctuations. This makes the experimental situations much more diverse than those for a 3D magnet.

We first consider the individual DW motion by formulating an effective equation of motion under the influence of the field $H(t)$, which we solve then in a finite geometry. This will lead us to the *characteristic fields* H_{t1}, H_{t2}, H_c, H_r and the HLA \mathcal{A} which we analyze in several limiting regimes in which simple power scaling is valid.

In general, the DW motion in an impure magnet is highly non-linear. However, as it was shown in [12,13], after integrating out DW fluctuations on time scales less than the dynamical correlation time t_v defined below, the effective equation of motion for the center of mass coordinate of the interface Z is given by

$$\dot{Z} \approx H_p \gamma f \left(\frac{H}{H_p} - 1 \right), \quad f(x) \approx \begin{cases} x^\theta, & x \ll 1 \\ x, & x \gg 1 \end{cases} \quad (1)$$

where γ represents the bare DW mobility. Inside the critical region $H - H_p \ll H_p$, $f(x)$ obeys a power law with an exponent θ of the order $1/3$ from an ϵ -expansion around five dimensions extrapolated to $d=2$ dimensions [12]. On time scales $t \gg t_v$ (i.e. for $\omega t_v \ll 1$), and length scales $L \gg \xi_v$ where $t_v \approx \frac{l}{\gamma H_p} \left(\frac{H}{H_p} - 1 \right)^{-\tilde{\nu}}$ and $\xi_v \propto \left(\frac{H}{H_p} - 1 \right)^{-\nu}$, fluctuations of the DW around its mean position are weak and will be neglected therefore in the following. Here ν and $\tilde{\nu}$ are the correlation length and time, respectively, exponent of the driven interface, with $\nu(d=2) = 1$ and $\tilde{\nu}(d=2) = 4/3$ again from an ϵ -expansion around five dimensions. Outside the critical region, $H \gg H_p$, $\theta = 1$ and the domain wall is macroscopically flat.

We solve now equation of motion for a planar DW which can move over a distance L forth and back. Here L corresponds to a characteristic size of the system. In the simplest case L denotes its linear extension. In some experiments only one domain wall survives and the model problem of rectilinear domain wall motion is close to reality. Another situation may occur in systems with rare, but strong extended defects. In passing such a defect domain walls may form bubbles of reversed spins. These bubbles play then the role of prepared nuclei in the next half-cycle of the magnetization reversal. In this case L can be identified with the mean distance L_{ed} between the extended defects. E.g. in random field magnets strong defects result from a coherent fluctuation of random fields on neighboring sites in which case L_{ed} is given by

$$L_{ed} \approx l \exp \left[\frac{c\Gamma}{(\eta - H_0)l} \right]^d \quad (2)$$

where $\eta > H_0$ and Γ denote the strength of the uncorrelated random field and the DW stiffness, respectively. Here $\Gamma/l \gg \eta \gg H_p$ and c is a constant of order unity.

The domain wall is assumed to be fixed at the left boundary of the sample $Z = 0$ at the initial moment. Solving equation of motion (1) for the domain wall coordinate Z in harmonically oscillating magnetic field, we replace the integration over time by the integration over the field, using $dt = \frac{1}{\omega} \frac{dH}{\sqrt{H_0^2 - H^2}}$. This yields

$$Z(H) = \frac{\gamma H_p}{\omega} \int_{H_p}^H f\left(\frac{H - H_p}{H_p}\right) \frac{dH}{\sqrt{H_0^2 - H^2}}. \quad (3)$$

This equation is correct for $H > H_p$. At smaller values of H the domain wall does not move. The sign of the square root changes each time as H reaches its maximum or minimum value $\pm H_0$. The second necessary prescription is to substitute $H - H_p$ by $-(H - H_p)$ in the argument of the function f and H_p by $-H_p$ in the lower limit of the integral (3) when H is negative. To transfer from the coordinate Z to the magnetic moment \mathcal{M} , we write $\mathcal{M}(Z) = \mathcal{M}_s(2Z - L)/L$. The area of hysteresis loop \mathcal{A} can now be expressed in integral form:

$$\mathcal{A} = 4H_p\mathcal{M}_s(1 - \frac{1}{LH_p} \int_{H_p}^{H_r} Z(H) dH). \quad (4)$$

For later applications, it is useful to introduce the functions $\Phi(a, b)$ and $\tilde{\Phi}(a)$ defined by

$$\Phi(a, b) = \int_1^a f(x-1) \frac{dx}{\sqrt{b^2 - x^2}}. \quad (5)$$

and $\tilde{\Phi}(a) = \Phi(a, a)$. Eq. (3) can then be rewritten in the form $Z/L = u^{-1}\Phi(H/H_p, v)$, where u and v are the two dimensionless variables

$$u = \omega L/(\gamma H_p), \quad v = H_0/H_p \quad (6)$$

It is clear, that the HLA \mathcal{A} also depends on these two parameters.

There are two important characteristic values for the amplitude H_0 which separate hysteresis loops of different shapes. The first of them is the *dynamic threshold field* H_{t1} , which is the smallest value of H_0 at which the domain wall reaches the right boundary of the sample $Z = L$. At $H_0 < H_{t1}$ the magnetization is not reversed fully, the hysteresis loop is asymmetric, whereas at larger values of H_0 the hysteresis loop is symmetric under inversion $H \rightarrow -H, \mathcal{M} \rightarrow -\mathcal{M}$ (Fig. 1). The value of H_{t1} is determined by solution of equation

$$\frac{\omega L}{2\gamma H_p} = \tilde{\Phi}\left(\frac{H_{t1}}{H_p}\right) \quad (7)$$

At $H_0 = H_{t1}$ the hysteresis loop is symmetric with respect to reflections in the axis H and \mathcal{M} . The second threshold field H_{t2} is defined as a value of H_0 at which the domain wall

reaches the right end of the sample $Z = L$ during one fourth of period, just at $H = H_0$. The definition of H_{t2} differs from Eq. (7) by the absence of factor 2 in denominator of the l.h.s. The hysteresis loops corresponding to $H_0 > H_{t2}$ acquire characteristic “mustaches”, single-valued pieces of the curve $\mathcal{M}(H)$, which are absent in hysteresis curves for $H_0 < H_{t2}$ (see Fig. 1d).

At a fixed $H_0 > H_{t1}$ it is possible to define the *coercive field* H_c by the requirement $\mathcal{M}(H_c) = 0$. The so-called *reversal field* H_r is defined as the field value at which the magnetic moment reverses fully. At $H = H_r$ the two branches of the hysteresis curve intersect each other, i.e. $Z(H_r) = L$. At H between H_r and H_0 the magnetic moment remains a constant $\mathcal{M} = \mathcal{M}_s$. The values H_c and H_r are shown in Fig. 1c,d. Using equation (3) and the relation for $\mathcal{M}(z)$, we find for H_c :

$$\frac{\omega L}{2\gamma H_p} = \Phi\left(\frac{H_c}{H_p}, \frac{H_0}{H_p}\right). \quad (8)$$

For $H_{t2} < H_0$ the relation for H_r differs from (8) by the absence of the the factor 1/2 in the l.h.s. For $H_{t1} < H_0 < H_{t2}$ the reversal field H_r is given by

$$\frac{\omega L}{\gamma H_p} = 2\tilde{\Phi}\left(\frac{H_0}{H_p}\right) - \Phi\left(\frac{H_r}{H_p}, \frac{H_0}{H_p}\right) \quad (9)$$

Thus, also the ratios H_c/H_p and H_r/H_p are functions of u and v only.

We analyze different asymptotics of the hysteresis loop characteristics starting with the simplest limiting case $u \gg 1$. In this case the contribution to $Z(H)$ from the critical region is negligible and no further restriction for the applicability of (1) apply. The main contribution to the integral (5) comes from large values of the argument and the function $\Phi(a, b)$ can be calculated explicitly by replacing $f(x - 1)$ by x and setting the lower cut-off for the integration equal to zero. This yields $\Phi(a, b) \approx b - \sqrt{b^2 - a^2}$. As a result H_p disappears from all expressions and a *new dimensionless parameter* $\tilde{u} = \omega L / (\gamma H_0)$ emerges. In particular we get for dynamic threshold field $H_{t1} \gg H_p$

$$H_{t1} = \frac{\omega L}{2\gamma} = H_{t2}/2. \quad (10)$$

Similarly, H_c and H_r are determined by $H_c = \sqrt{H_{t1}(2H_0 - H_{t1})}$ and $H_r = \sqrt{H_{t2}(2H_0 - H_{t2})}$. The shape of the HL for $H_0 > H_{t2}$ is described by

$$\mathcal{M} = \mathcal{M}_s \left[1 - 2\tilde{u}(1 - \sqrt{1 - (H/H_0)^2}) \right]. \quad (11)$$

It can be used also for the range of amplitudes $H_{t1} < H_0 < H_{t2}$ on the lower branch of the hysteresis curve $0 < H < H_0$. On the upper branch of this curve $H_r < H < H_0$ the sign of the square root must be reversed. If $H_0 > H_{t2}$, the HLA is determined as follows:

$$\frac{\mathcal{A}}{4\mathcal{M}_s H_r} \approx 1 - \tilde{u} + \frac{\tilde{u} \arcsin \frac{H_r}{H_0}}{2\sqrt{1 - (\frac{H_r}{H_0})^2}} + \frac{\tilde{u}}{2} \sqrt{1 - (\frac{H_r}{H_0})^2}. \quad (12)$$

On the contrary, for $H_0 < H_{t2}$, the area is:

$$\mathcal{A} = 4\mathcal{M}_s H_r (1 - \tilde{u}) + \pi \mathcal{M}_s H_0 \tilde{u}. \quad (13)$$

In the range of existence of the full HL $\tilde{u} < 1/2$. Therefore \tilde{u} cannot be large. However it can be very small, i.e. $\omega L \ll \gamma H_0$. In this case we find $H_r \approx H_c = H_0 \sqrt{\tilde{u}} = \sqrt{\omega L H_0 / \gamma}$, $\mathcal{M}(H) = \mathcal{M}_s (1 - 2H^2/(\tilde{u}H_0^2))$ and

$$\mathcal{A} \approx 4\mathcal{M}_s H_r \propto \omega^{1/2} H_0^{1/2}. \quad (14)$$

Thus, for $\tilde{u} \ll 1$ we find the scaling behavior of all hysteresis characteristics with universal critical exponents, independent on the pinning centers. Therefore, one can expect that the same scaling is valid for a clean ferromagnet with the relaxational dynamics.

Next we study the opposite limit of small $u \ll 1$. In this case H_{t1} and H_{t2} are close to H_p as follows from (7), (8), (9). Solving the integral (5) approximately and employing for $f(x)$ at small x (1), we get

$$\Phi(a, b) \approx \frac{(b-1)^{\theta+1/2}}{\sqrt{2}} B(\theta+1, \frac{1}{2}, \frac{a-1}{b-1}) \quad (15)$$

where we introduced the incomplete B -function defined by the integral

$$B(x, y, z) = \int_0^z s^{x-1} (1-s)^{y-1} ds \quad (16)$$

In particular, we get $\tilde{\Phi}(a) \approx \sqrt{\frac{\pi}{2}}(a-1)^{\theta+1/2} \frac{\Gamma(\Theta+1)}{\Gamma(\Theta+3/2)}$. One then finds from (7) for H_{t1}

$$\frac{H_{t1}}{H_p} - 1 \approx \left[\frac{(1 + 1/2\theta)\Gamma(\theta + 1/2)}{\sqrt{2\pi}\Gamma(\theta)} \frac{\omega L}{\gamma H_p} \right]^{\frac{2}{2\theta+1}}. \quad (17)$$

H_{t2} is given by the same expression if we replace L by $2L$ in (17). The ratio $(H_{t2} - H_p)/(H_{t1} - H_p) = 2^{2/(2\theta+1)}$ does not depend on u . We omit here the explicit expressions for H_c and H_r but give finally the results for the HLA in the case $u \ll 1$. For (i) $v - 1 \ll 1$ we get:

$$\frac{\mathcal{A}}{4\mathcal{M}_s H_p} \approx 1 + \frac{\sqrt{2}(v-1)^{\theta+1/2}}{u} \int_0^w B(\theta+1, 1/2; x) dx. \quad (18)$$

where $w = (H_r - H_p)/(H_0 - H_p)$. In the case (ii) $v \gg 1, uv \ll 1$ we find:

$$\mathcal{A} \approx 4\mathcal{M}_s H_p \left[1 + \frac{((\theta+1)uv)^{1/(\theta+1)}}{\theta+2} \right]. \quad (19)$$

Finally, for (iii) $uv \gg 1, H_r \gg H_p$ and therefore all essential results formally coincide with those for $u \gg 1$. In the cases (i) and (ii) \mathcal{A} is close to $\mathcal{A}_0 = 4\mathcal{M}_s H_p$ but the deviation $\mathcal{A} - \mathcal{A}_0$ scales with the parameters u and v . The prerequisite inequalities $\omega t_v \ll 1$ and $\xi_v \ll L$, lead for $u \ll 1$ to further restrictions on L and ω , which in general can be fulfilled if L is large enough [11].

We have also used Monte-Carlo simulation with Glauber dynamics to check (1), (11) and (14) for a random bond Ising model. The disorder has weak influence on phase diagram, but decreases significantly the DW velocity. However, no measurable pinning threshold field H_p has been detected. To separate domain growth from domain nucleation we have studied two different cases: (i) specially prepared defects for fast nucleation, (ii) generated nucleus with the opposite direction of magnetization in the form of circle or stripes. The magnetization changed according to the model of a straight DW, i.e. similar to Eq. (11). In this case usually one or two domains inflate from the nucleation centers. The distance L_N between nucleation centers play the role similar to the system size L in the above consideration. We have studied scaling behavior of HLA \mathcal{A} (see Eq. 14) for the case when it is determined by the domain growth. Details will be published elsewhere [11]. We found scaling $\mathcal{A} \propto \omega^\beta$ with $\beta = 0.49 \pm 0.05$ over three decades of ω . However the range of H_0 values available is only

one decade. For this reason we have only checked that the dependence is consistent with $\mathcal{A} \propto H_0^{1/2}$.

To conclude, we have studied the hysteresis process in controlled by the DW motion. We introduced two dynamical threshold fields H_{t1} and H_{t2} corresponding to the occurrence of the full magnetization reversal and to the occurrence of the single-valued parts on the hysteresis curve respectively. These dynamical threshold fields are larger than the static threshold field H_p which is required to start the motion of the DW. We established that H_{t1} and H_{t2} expressed in units H_p are functions of one dimensionless parameter $u = \omega L/\gamma H_p$. The coercive field H_c and the reversal field H_r expressed in the same units are function of two dimensionless parameters $H_c = H_p F\left(\frac{\omega L}{2\gamma H_p}, \frac{H_0}{H_p}\right)$ and $H_r = H_p F\left(\frac{\omega L}{\gamma H_p}, \frac{H_0}{H_p}\right)$. Experimental observation of this type of scaling would be the best indirect evidence of the DW motion controlled hysteresis. A direct observation of the DW motion in principle is possible [14]. At large fields $H_0 \gg H_p$ the defects are inessential. Therefore the dependence on H_p must vanish from all scaling laws. It happens indeed, and both fields H_c and H_r are expressed in terms of one dimensionless parameter $\omega L/\gamma H_0$. We presented also corresponding equations for the HLA to which the most experimental efforts were concentrated. However, we would like to emphasize that the HLA is not the only measurable characteristics of the HL and even not the most informative of its characteristics: the fields H_{t1}, H_{t2}, H_c, H_r as well as the shape of the hysteresis curve are not less interesting. In the case when the driven DW are almost free ($H_0 \gg H_p$) and the HL is narrow ($H_0 \gg H_{t1}$) the HLA was found to be proportional to $\omega^{1/2} H_0^{1/2}$. This conclusion is supported by our numerical MC simulation.

Acknowledgments. This work was partly supported by the grants DE-FG03-96ER45598, the SFB 341 and the GIF. V.P. is thankful to Prof. J. Zittartz for the hospitality extended to him during his stay at Cologne University.

REFERENCES

* Also at Institute of Physics, 252028 Kiev, Ukraine

- [1] C.P.Steinmetz, Trans.Am.Inst.Electr.Eng. **9**, 3 (1892).
- [2] W.S.Lo and R.Pelcovits Phys.Rev.A **42**, 7471 (1990).
- [3] D.Dhar and P.B.Thomas, J.Phys.A **25**, 4967 (1992).
- [4] M.Acharyya and B.K.Chakrabarti, Physica A **192**, 471 (1993); Phys.Rev.B **52**, 6550 (1995).
- [5] C.N.Luse and A.Zangwill, Phys.Rev.E **50**, 224 (1994).
- [6] Y.L.He and G.C.Wang, Phys.Rev.Lett. **70**, 2336 (1993).
- [7] Q.Jiang, H.-N.Yang, and G.C.Wang, Phys.Rev.B **52**, 14911 (1995).
- [8] J.-S.Suen and J.L.Erskine Phys.Rev.Lett. **78**, 3567 (1997).
- [9] P.Bruno, G.Bayreuther, P.Beauvillain, C.Chappert, G.Lugert, D.Renard, J.P.Renard, and J.Seiden, J.Appl. Phys. **68**, 5759 (1990).
- [10] B.Raquet, R.Mamy, and J.C.Ousset Phys.Rev.B **54**, 4128 (1996).
- [11] I.F.Lyuksyutov, T. Nattermann and V. Pokrovsky, subm. to Phys.Rev. B
- [12] T. Nattermann, S. Stepanow, L.-H. Tang, H. Leschhorn, J. Phys. II France **2** (1992) 1483
- [13] O. Narayan, D. S. Fisher, Phys. Rev. B, **48** (1993) 7030
- [14] L.H.Bennett, R.D.McMichael, L.J.Swartzendrubler, S.Hua, D.S.Lashmore, A.J.Shapiro, V.S.Gornakov, L.M.Dedykh, V.I.Nikitenko, IEEE Trans.Mag. **31** (1995) 4088

FIGURES

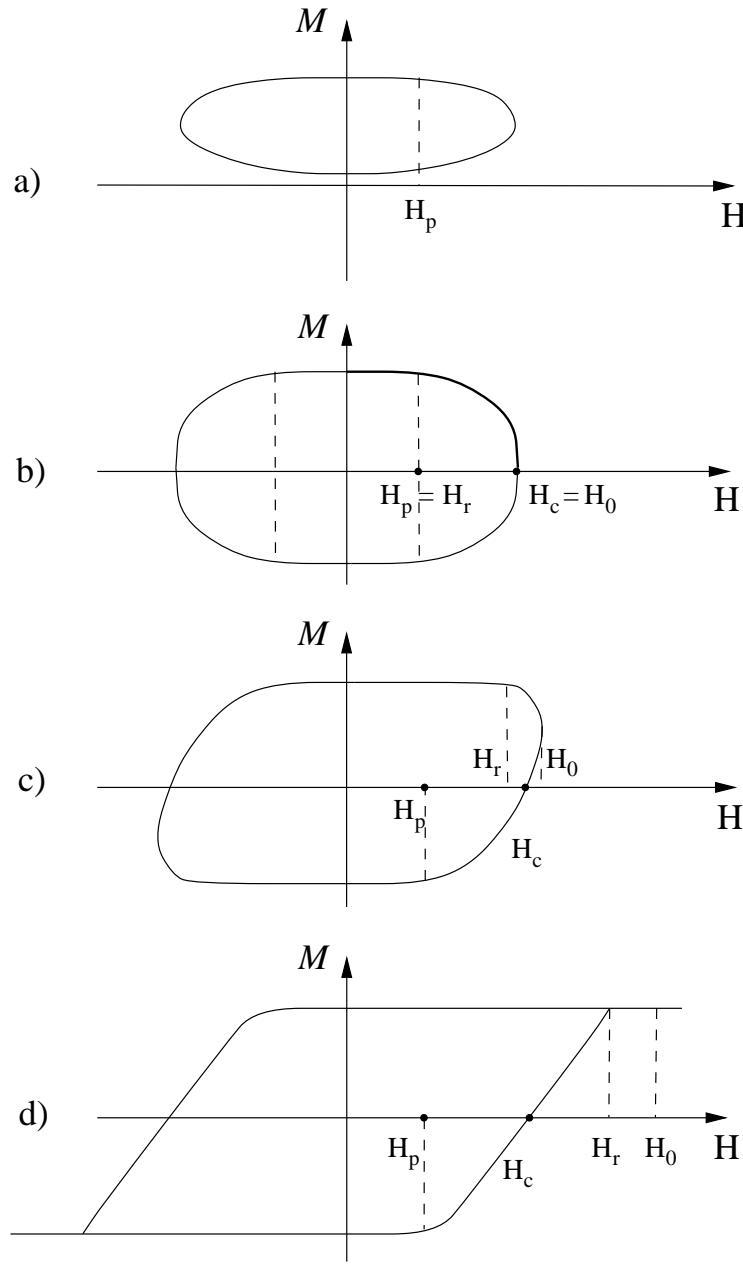


FIG. 1. Schematic pictures of hysteresis loops.

(a) Incomplete HL for $H_0 < H_{t1}$.

(b) Symmetric HL for $H_0 = H_{t1}$.

(c) The HL for $H_{t1} < H_0 < H_{t2}$.

(d) The HL for $H_0 > H_{t2}$.

The values H_p , H_c , H_r , H_0 are marked in all figures.